Structural Steel as Boundary Elements in Ductile Concrete Walls

Cho, Soon-Ho*

Abstract

A new form of construction utilizing structural steel as the boundary elements in ductile flexural concrete walls is proposed to solve the bar congestion problems in such a heavily reinforced region, while maintaining the ductility and energy absorption capacity comparable to their traditional form. Two wall specimens containing rectangular hollow structural sections (HSS) and channels at their ends respectively, and one companion standard reinforced concrete wall specimen with concentrated end reinforcement were constructed and tested under reversed cyclic loading to evaluate the construction process as well as the structural performance. Initially, all three specimens were chosen and detailed with some caution to have approximately the same flexural capacity without change of the original shape and dimension of a rectangular cross section correction. Analysis and comparison of test results indicated that the reversed cyclic responses of three walls showed similar hysteretic properties, but in those with steel boundaries, local buckling of the corresponding steel webs and flanges following significant yielding was a dominant factor to determine the hysteretic response. The monotonic and cyclic responses predicted based on a sectional approach was also presented and found to be in good agreement with measured results. Design recommendations considering local instability of the structural steel elements and the interaction between steel chords and a concrete web member in such a composite wall are presented.

Keywords : composite wall, concrete, confinement, ductility, flexure, hysteresis loop, local buckling, structural steel

* KCI Member, Professor, Dept. of Architectural Engineering, Kwangju Univ., Kwangju, Korea.

1. Introduction

Providing a significant amount of confining reinforcement at the compressed edges of ductile flexural concrete walls to ensure the high deformation capacity is a common practice in earthquake resistant-design of reinforced concrete structures[1]. However, this often causes serious difficulty in the bar placement due to the smaller spacing required, and is sometimes not possible in Korean situation because very thin walls are normally adopted for residential buildings. Examining the possibility of replacing the conventional reinforcement by structural steel in such heavily reinforced regions is a core issue of this research. This way of construction has many advantages such as the reduction of on-site labor related to the bar placement, easy connection to steel frames in case of mixed construction used, and steel end members also acting as the permanent formwork. Furthermore, some inherent properties related to composite members such as the increased strength, stiffness and energy absorption are expected, but they are not yet in a usable form for design purposes[2]. The research reported herein aims at investigating the reversed cyclic loading responses of alternative construction techniques, incorporating structural steel boundary elements interconnected to the reinforced concrete web of the wall, by comparisons with that of an ordinary concrete wall with conventional reinforcement details.

2. Experimental Programme

Three half scale test specimens from a twelve storey prototype structure were designed and detailed according to the requirements of the force modification factor, R=3.5, in the Canadian Concrete and Steel Codes[3, 4]. The value of R used in Canadian codes has the maximum value of 4.0, so that its relative magnitude in the Korean Code[5] can be estimated. At an initial stage, the details of three walls were carefully chosen such that all of the walls had approximately the same flexural capacity. The complete interaction between structural steel and concrete in composite wall specimens was also ensured. Due to the available testing apparatus, the wall specimens were tested in their horizontal positions as shown in Fig. 1. The constant axial load of 600kN corresponded to approximately 11% of the gross sectional concrete strength. A steel frame near the tip of the wall was also used to prevent out-

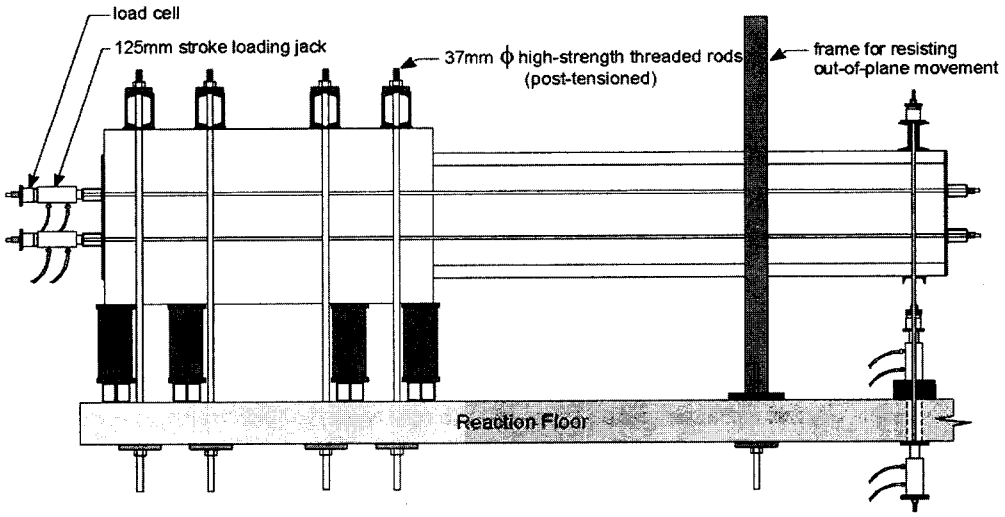

Fig. 1 Test setup

of-plane movement of the wall.

Fig. 2 shows the overall and cross-sectional dimensions, and structural steel and reinforcement details of the three test specimens. The cross-sectional dimensions of each wall were 1000mm by 152mm, with the wall cantilevering 3900mm from the end foundation block.

Specimen W1 used rectangular hollow structural sections (HSS) as boundary elements, which were connected to the wall by welding the transverse bars directly to both HSS elements. The HSS sections were not filled with concrete. Specimen W2 had steel channels connected to the wall with headed studs, which were welded to the channels and overlapped 175mm with the transverse reinforcing bars having headed ends of 37mm x 37mm x 9.5mm plates. Specimen W3 is a companion test that meets the requirements of a standard reinforced concrete ductile flexural wall. The confining ties were spaced at a distance of one half the wall thickness, 76mm, in the plastic hinge region and were spaced at 152 mm elsewhere.

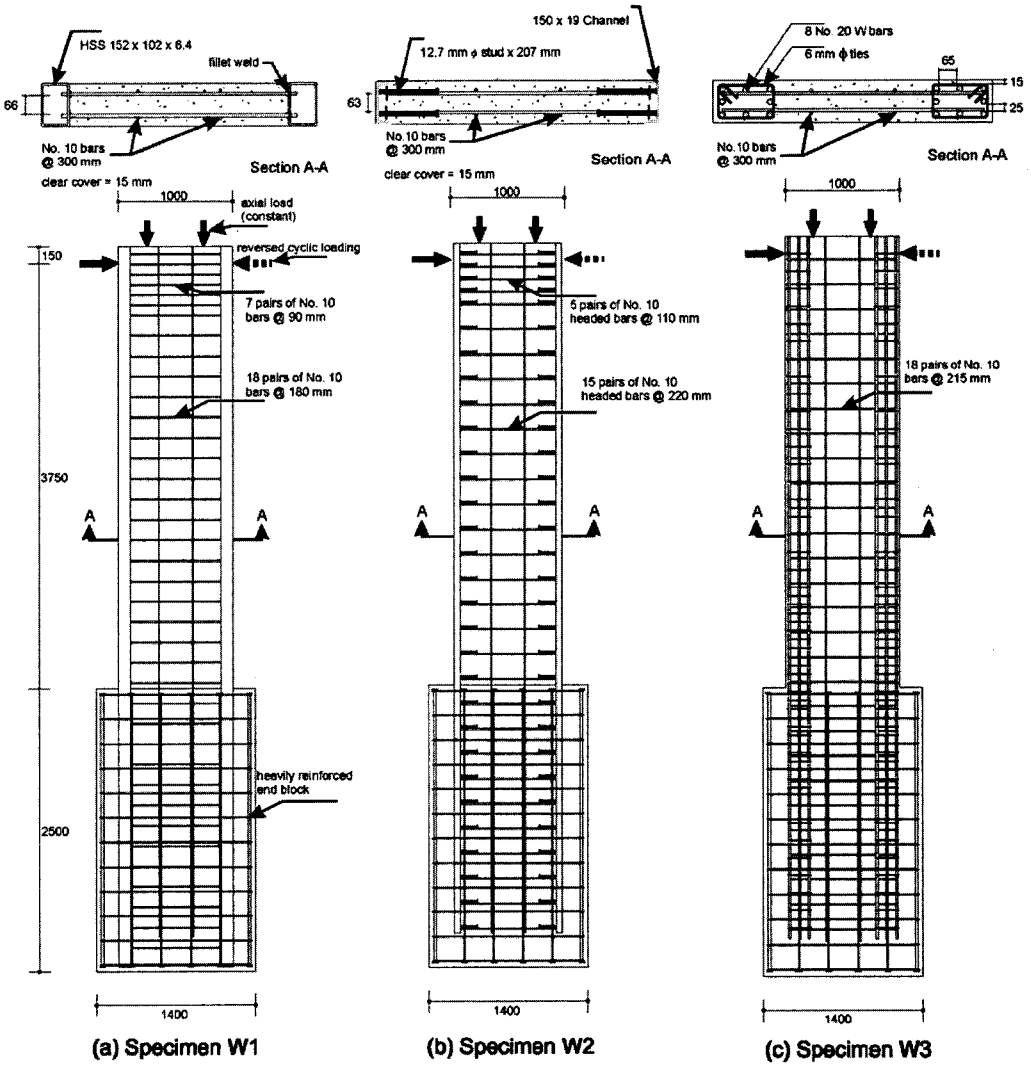

Fig. 2 Details of test specimens

The construction sequence of Specimen W1 was to drill holes in the HSS elements first, then place the bars and align the steel sections, and finally weld to the transverse bars. In Specimen W2, the transverse bars were fabricated by welding plates to their ends resulting in headed bars, 930mm in length. Standard stud welding procedures were used, which enabled the rapid welding of the studs to the channel boundary elements.

The properties of reinforcing bars are given in Table 1, and also those of the two types of structural steel and the studs are summarized in Table 2. According to the ratios of width-to-thickness in flanges and height-to-thickness in webs, the flange of a HSS and the web of a channel are more susceptible to local buckling. The effective slenderness ratios, which are a function of the transverse reinforcement or shear connector spacing, s_h are also given. The average concrete strengths used for Specimen W1, W2 and W3 were 25.8 MPa, 38.1 MPa and 38.7 MPa respectively.

Table 1 Properties of reinforcing steel

Bar size	Bar description	f_y, Mpa	ε_y, mm /mm	f_{ult}, Mpa
6 mm diameter	W3 confining hoops	381.2	0.00174	445.2
No. 20	W3 flexural reinforcement	450.1	0.00246	610.0
No. 10	Distributed reinforcement	487.8	0.00285	597.5

Table 2 Properties of structural steel

Property	Specimen W1	Specimen W2
Steel Description (Area, mm^2)	HSS 152x102x6.4 (2960)	C 150x19 (2450)
F_y, MPa	377.0	402.2
ε_y, mm/mm	0.00500	0.0028
F_{ult}, MPa	442.5	555.0
Flange b/t ratio = (b-2t)/t	21.9	12.1
CSA Class 1 Flange*, b/t limit	$21.6_{(420/\sqrt{F_y})}$	$20.9_{(420/\sqrt{F_y})}$
Web h/w ratio	14.1	6.2
CSA Class 1 Web*, h/w limit	$21.6_{(420/\sqrt{F_y})}$	$7.2_{(145/\sqrt{F_y})}$
s_h, mm	180	220
Effective slenderness ratio = s_h/t	28.3	19.3
Studs in Specimen W2 (12.7mm diameter and 207mm length)		
F_y, MPa	402.0	
F_{ult}, MPa	500.7	

* flange and web are longer and shorter elements respectively

Load cells were used to measure the positive (downwards) and negative (upwards) shear forces on each wall and to monitor the axial load. A number of linear voltage differential transducers (LVDTs) were used to measure the deflections at various locations of each wall. Strain measurements were collected using both electrical resistance strain gauges and demountable mechanical targets. Typical assemblies of LVDT and strain gauges used are shown in Fig. 3(a) and (b).

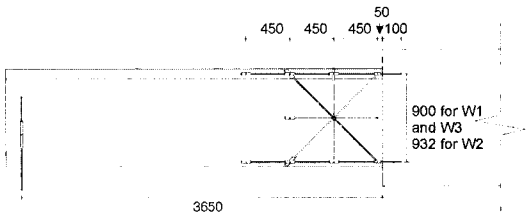

(a) LVDT Assembly (view of back side of wall)

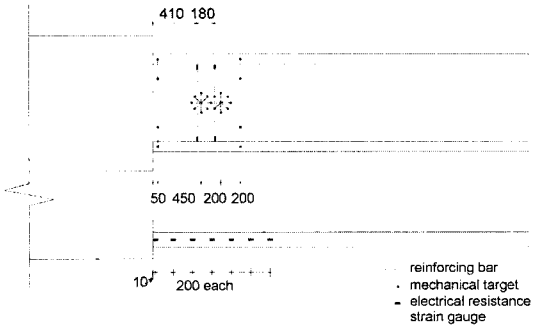

(b) Strain Measuring Instrumentation

Fig. 3 Typical measurement setup

Loading was applied to predetermined load levels up to the general yielding. The first cycle was to produce the precalculated moment, $0.5M_{cr}$, equal to half of the cracking moment. The second cycle loaded the walls to the theoretical cracking moment, M_{cr}. The next cycle was determined by the first yielding of flexural steel in the wall, monitored by the electrical resistance strain gauges. The peak of the fourth cycle was taken as the load and deflection corresponding to general yield, Δ_y, of the wall. The cycles after general yielding were controlled by deflection limits, based on multiples of the general yield deflection.

3. Experimental Results

Fig. 4 shows the base moment vs. wall tip deflection responses for the three specimens, indicating similar hysteretic behaviour. The key features observed during each test are also summarized in Tables 3, 4 and 5.

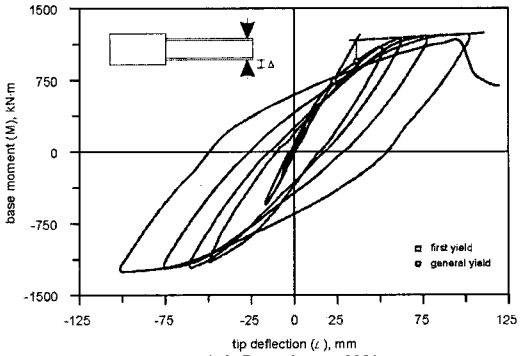

(a) Specimen W1

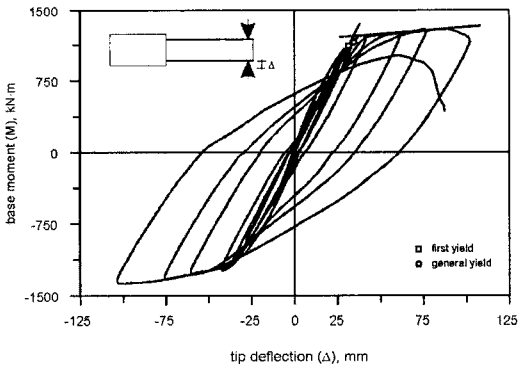

(b) Specimen W2

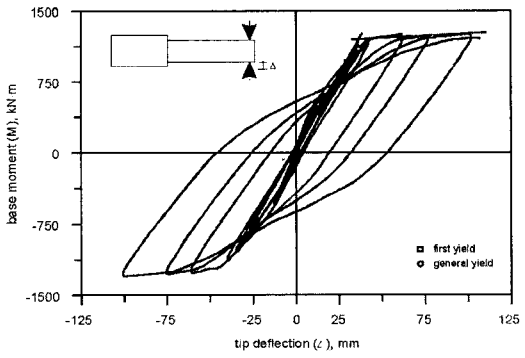

(c) Specimen W3

Fig. 4 Moment vs. deflection responses

Table 3 Salient features observed for specimen W1

Cycle	Cycle Description	Observations
2A 2B	2.0 M_{cr}+ 2.0 M_{cr}-	First yielding (Δ=22mm, V=191.2kN).
3A' 3A 3B' 3B	Δ_y $1.4\Delta_y$ Δ_y $1.5\Delta_y$	General yielding (Δ_y=36.6mm, V_y=257.5kN), significant flexural cracks at location of transverse bars.
4A 4B	$1.7\Delta_y$ $1.8\Delta_y$	Crushing of concrete near base.
5A 5B	$2.1\Delta_y$ $2.0\Delta_y$	Sign of local bucking in outer flanges.
7A	$3.3\Delta_y$	Excessive crushing, complete buckling and failure.

Table 4 Salient features observed for specimen W2

Cycle	Cycle Description	Observatio.ns
4A 4B	$<M_y$ M_y	First yielding (Δ=-30.9mm, V=-279.8kN).
5A 5B' 5B	$0.97\Delta_y$ Δ_y $1.1\Delta_y$	General yielding (Δ_y=-33.7mm).
6A' 6A 6B	Δ_y $1.2\Delta_y$ $1.3\Delta_y$	Horizontal along concrete and steel interface.
7A 7B	$1.8\Delta_y$ $1.8\Delta_y$	Significant flexural cracks and first noticeable concrete crush- ing, pullout of steel section.
9A 9B	$3.0\Delta_y$ $3.1\Delta_y$	Sign of local buckling, crush- ing and spalling , several large shear cracks
10A	$2.5\Delta_y$	Severe buckling and failure.

maximum shear capacity followed by in the order of concrete crushing, compression yielding and local instability of steel chords near the base of the wall. As can be seen in Fig. 5(a) and (b), many flexural cracks were formed at the location of each shear connection, and a series of shear cracks was developed propagating from these flexural cracks.

Table 5 Salient features observed for specimen W3

Cycle	Cycle Description	Observations
4A 4B	$0.8\Delta_y$ $0.8\Delta_y$	First yielding (Δ=28mm, V=251.2kN), First shear cracks, Compres- sion yielding of rebar.
5A 5B	Δ_y $0.9\Delta_y$	General yielding (Δ_y=35.8mm).
6A 6B' 6B	$1.2\Delta_y$ Δ_y $1.1\Delta_y$	Significant shear cracks.
7A 7B	$1.7\Delta_y$ $1.6\Delta_y$	Sign of concrete crushing.
8A 8B	$2.1\Delta_y$ $2.0\Delta_y$	Severe shear cracks and sig- nificant crushing.
10A	$3.2\Delta_y$	Severe distress in compression zone, rupturing of one tie and local buckling of rebars, and failure.

No significant separation at the interfaces between concrete and steel sections was observed in specimen W2, while significant separations of 1mm towards the end of testing were indicated by mechanical targets readings in specimen W2. The transverse reinforcement in the plastic hinge region in both specimens corresponded to 80% and 50% of their yield strains at failure respectively. Once local buckling was noticeable, both composite wall specimens began to exhibit severe strength and stiffness degradation.

Specimen W1 and W2 reached at the Specimen W3 was failed due to severe distress in the compression zone, with concrete crushing, rupturing of one of the confining ties and local buckling of the longitudinal bars. The crack pattern of specimen W3 was significantly different from those of specimens W1 and W2 as can be seen from Fig. 5(c), a large number of closely spaced small cracks in the area of the concentrated longitudinal reinforcement, and shear cracks merged thereafter.

(a) Specimen W1

(b) Specimen W2

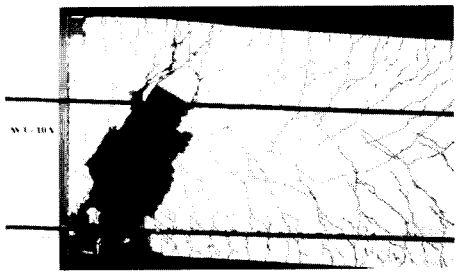

(c) Specimen W3

Fig. 5 Crack patterns and failure modes

Significant shear strains were measured in the plastic hinge region, but neither the transverse nor confining bars yielded until failure. Close-up views of local buckling related to each specimen can be seen from Fig. 6. For more details, reference be can be made elsewhere[6].

4. Analysis and Prediction of Responses

The analysis of the reversed cyclic responses, behavioural comparisons and a discussion of the differences in the construction techniques for the three wall specimens are presented.

The construction of concrete walls with steel boundary elements proved to have several advantages. Among them, the major advantage is that considerable prefabrication is possible, reducing the on-site labour and hence reducing construction time. Specimen W1 required a significant amount of welding and drilling which necessitated more labour than was needed for Specimen W2. Combining studs and prefabricated headed reinforcing bars was a concept that made Specimen W2 a reasonable alternative to conventional construction.

Fig. 7 presents the moment vs. curvature responses, determined from the curvatures measured near the base and the corresponding moments for each wall. Monotonic responses for each wall were also predicted using the computer

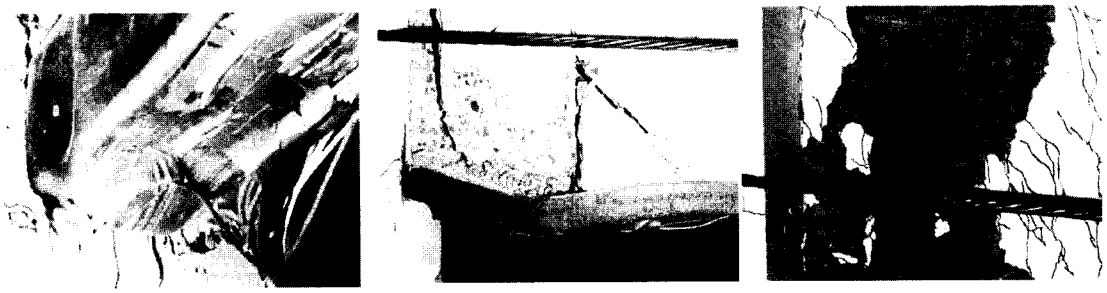

(a) (b) (c)

Fig. 6 Close-up views of failure regions

programs RESPONSE[7]. The cross-section of each wall was discretized into ten concrete layers with the boundary elements simulated by several steel layers. The full non-linear responses of both the concrete and the steel, including strain hardening and confining effects were modelled [8].

On the other hand, the hysteresis loop of each wall was predicted using a shear element given by IDARC[9] that is based on the fiber element approach and includes versatile options of strength and stiffness degradation parameters. As can be seen in Fig. 8, both the ultimate strength and stiffness observed in each wall were closely captured before local buckling of structural steel came into play significantly.

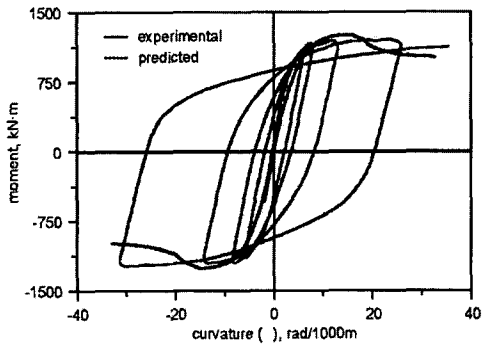

(a) Specimen W1

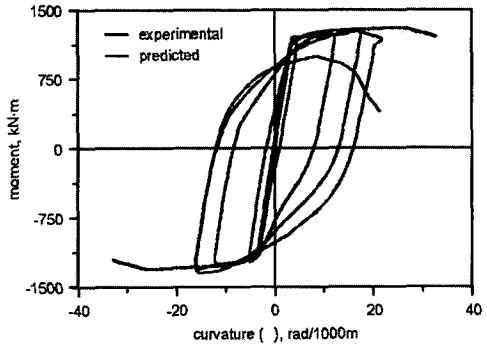

(b) Specimen W2

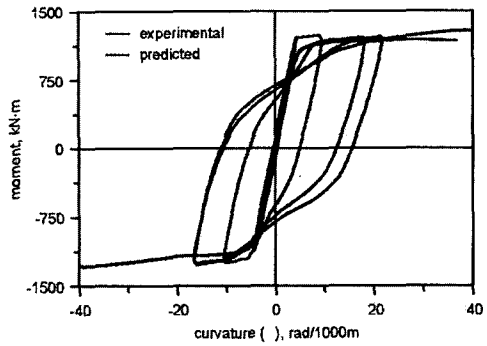

(c) Specimen W3

Fig. 7 Moment vs, curvature responses

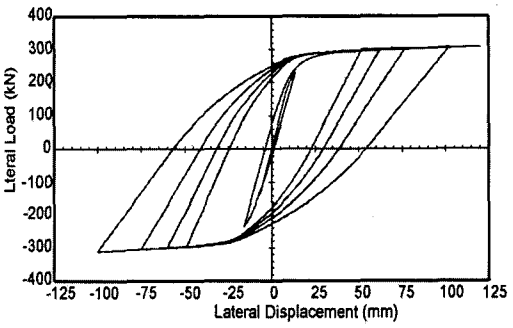

(a) Specimen W1

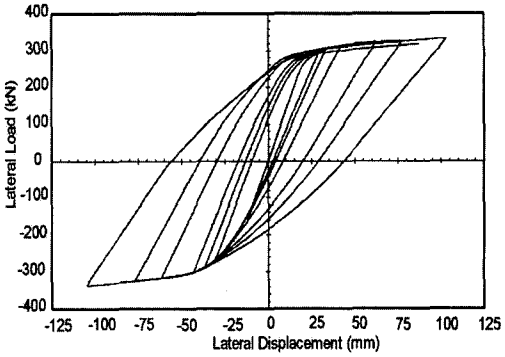

(b)Specime W2

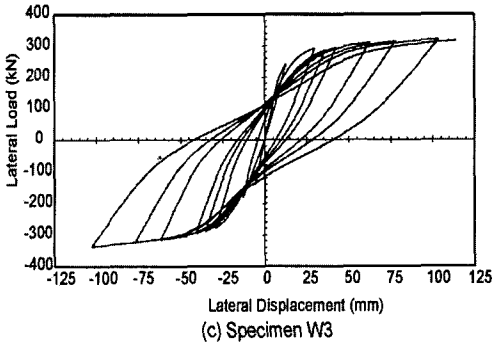

(c) Specimen W3

Fig. 8 Predicted hysteretic responses

The predicted curvatures are very close to the envelope of the experimental results. Table 6 summaries the predicted plastic hinge lengths determined from the assumed curvature distribution at ultimate stages and length of tension steel yielding determined from the electrical resistance strain gauges for three specimens. It must be noted that the actual plastic hinge length is somewhat less than the length over which yielding of the tension steel was recorded.

The hysteretic responses of the wall specimens are described using comparisons of the displacement ductility, ability to increase load beyond general yielding, peak-to-peak stiffness degradation and cumulative energy absorption. Table 7 summarizes the maximum values of each of these attributes and indicates the failure mode of each specimen. The deflection ductility is taken as the ratio of the ultimate positive tip deflection, Δ_u, to the positive tip deflection at general yield, Δ_y. The V_u/V_y ratio indicates a specimen's ability to increase its load and maintain the load after general yielding. V_u and V_y represent the loads corresponding to Δ_u and Δ_y, respectively. The third parameter, k_u/k_y, represents the stiffness degradation between general yielding and ultimate deflection.

The stiffnesses, k_u and k_y, represent the slope of the line joining the peaks of the respective positive and negative load-deflection responses. The cumulative energy dissipation is obtained by integrating the areas under the load-deflection curves and hence is representative of the hysteretic damping.

All three specimens have comparable displacement ductilities, averaging about 3.0. Table 4 and Fig. 9(a) show that Specimen W1 reached the largest value of V_u/V_y, since the response of this wall was governed by the structural steel. These tension and compression chords experienced significant strain hardening allowing Specimen W1 to maintain the load in the later stages. Specimen W2 began to lose its capability to sustain load in the last full cycle due to concrete crushing and buckling of the channel in compression. Specimen W3, after yield, maintained a constant V_{peak}/V_y ratio of approximately 1.1.

The ultimate stiffness ratios in Table 7 show that all of the specimens had a similar peak-to-peak stiffness ratio, k_u/k_y, at the end of their respective tests. Fig. 9(b) illustrates the stiffness degradation of each specimen throughout the entire test. The most evident difference between

Table 6 Predicted plastic hinge lengths and experimental yielding lengths

Specimen	M_y, kN·m	M_u, kN·m	L_p, mm	Yielding length, mm (from tests)
W1	986.5	1253.4	798	1200
W2	1079.8	1305.2	647	800
W3	1109.2	1285.0	513	750

Table 7 Summary of specimen responses

Specimen	Mode of failure	Δ_u/Δ_y	V_u/V_y	k_u/k_y	Energy, kN·m
W1	HSS local buckling	2.80	1.27	0.42	71.0
W2	Channel local buckling And concrete crushing	3.0	1.03	0.36	87.1
W3	Concrete spalling and crushing Followed by bar buckling and Rupture of confining ties	3.18	1.08	0.47	70.6

the specimens is the significantly lower initial stiffness of Specimen W1. Although Specimen W1 had comparable flexural strength to that of the other specimens its elastic stiffness was less due to the HSS being remained hollow. Fig. 9(c) compares the cumulative energy dissipation versus ductility for each wall. It is shown that Specimen W2 dissipated the greatest amount of energy, approximately 25% more energy than the other two specimens. The greater cumulative energy dissipation of Specimen W2 is due to the properties of structural steel and the filling of concrete to the interior of channels.

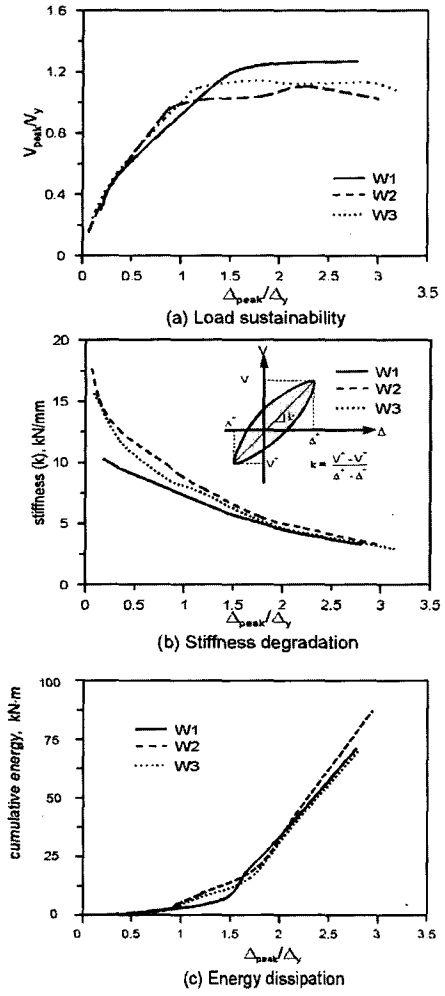

Fig. 9 Hysteretic responses

5. Structural Steel Local Buckling

Various types of structural steel sections such as wide-flange, angle, channel and HSS can be used for the chord members of composite walls. An HSS is one of the most economical sections because it is capable of developing large compressive strains. This is due to a larger radius of gyration when compared with other sections with the same cross sectional areas. However, there are concerns about the ductility of HSS brace members after local buckling occurs. HSS members serving as truss chords in a composite wall are expected to be subject to much less severe strain gradients over their depth. As described in Table 2, the width-to-thickness ratios in flanges and the height-to-thickness ratios in webs of the structural steel used all satisfy the requirements for Class 1 sections in the CSA S16.1 Standard[4]. The strain measurements on the steel sections included local strain measurements using electrical resistance strain gauges and average strain measurements using LVDTs. The electrical resistance strain gauges were typically located just outside of the regions of most severe local buckling, however the LVDT readings captured the average strains across these regions. From the strain readings the following conclusions were made: 1) Initial signs of local buckling are apparent at strains of about 1%, 2) Both the HSS and the channel sections had strains greater than 2% and hence it is assumed that strain hardening was achieved prior to local buckling. These reversed cyclic loading tests have indicated that in order for composite walls to exhibit comparable behaviour to a reinforced concrete ductile flexural wall, Class 1 sections must be used, since local buckling must be delayed until reasonably high strains are reached. Another important aspect in the design is to provide adequate connection between the steel section and the concrete. The provision of a

sufficient number of discrete shear connectors, such that their shear capacity would enable yielding of the HSS chord member, was found to be essential in achieving ductile response. This also results in the reduced effective slenderness ratio, s_h/t.

6. Summary and Conclusions

1) The hysteretic responses of composite walls with boundary elements were very similar to that of a typical reinforced concrete ductile flexural wall when all of the walls were designed to have equivalent flexural capacities. Composite wall Specimen W2 exhibited slightly better energy dissipation than the other two specimens.
2) The welding of transverse reinforcing bars directly to the hollow structural steel tubes in Specimen W1 provided excellent shear connection enabling the full development of yielding of the boundary elements. The shear connection in Specimen W2, consisting of studs welded to the steel channels together with overlapping headed transverse bars, proved capable of developing the full yield of the steel channels. However, significant separation occurred between the steel channel and the reinforced concrete web.
3) The failure mode of composite walls was precipitated by local buckling of the structural steel boundary elements. While a more compact steel section and a reduced spacing of shear connectors in the plastic hinge region would help control local buckling, both composite walls achieved ductilities and energy absorption comparable to the reinforced concrete ductile flexural wall.
4) The positioning of channels in Specimen W2 provided some concrete confinement at both ends of the wall. The placement of the hollow steel sections at the extreme ends of Specimen W1 enabled this wall to resist flexure almost entirely by forces in the structural steel chords.
5) The use of prefabricated elements in the construction of the boundary element walls would significantly reduce on-site labour. The construction of Specimen W1 required more care during prefabrication of the reinforcement than Specimen W2. However, Specimen W2 requires more on-site placement of reinforcement than Specimen W1. Due to the intricate details of the confinement reinforcement at the ends of Specimen W3, this specimen requires the greatest amount of on-site labour.

Acknowledgements

The authors would like to acknowledge STRESS, a nationwide research center in Korea which is in turn supported by KOSEF (Korean Science and Engineering Foundation) for funding this collaborative research project between STRESS and Concrete Canada.

References

1. Paulay, T., and Priestley M.J.N., Seismic Design of Reinforced Concrete and Masonry Buildings, John Wiley & Sons, New York, 1992.
2. Building Seismic Safety Council, "NEHRP Recommended Provisions for Seismic Regulations for New Buildings and Other Structures," Washington, D.C., 1997.
3. Canadian Standards Association, "CSA Standard A23.3-94-Design of Concrete Structures," Rexdale, Ontario, 1994.
4. Canadian Standards Association, "CAN/CSA-S16.1-Limit States Design of Steel Structures," Rexdale, Ontario, 1994.
5. The Ministry of Construction, "Korean Building Code," Seoul, 1988.
6. Cho, S. H., Lee, L. H., Tupper B. and Mitchell D., "Ductile concrete walls with steel ends,"

Paper No. 378/6/A, Proc., 12th World Conf. on Earthquake Engineering, EQC, Auckland, New Zealand. 2000

7. Collins, M.P., and Mitchell, D., "Prestressed Concrete Structures," Prentice Hall, Toronto /Montreal, 1997.
8. Mander, J. B., Priestley, M. J. N., and Park R., "Theoretical Stress-Strain Model for Confined Concrete," *ASCE Journal of Structural Engineering*, Vol. 114, No. 8, August, 1988, pp. 1804-1827.
9. Valles R. E., Reinhorn A. M., Kunnath S. K., and Madan A. (1996). "IDARC 2D Version 4.0: A program for the Inelastic Damage Analysis of Buildings," *Technical Report NCEER-96-0010*, National Center for Earthquake Engineering Research, State University of New York at Buffalo.